

Increasing Human Neural Stem Cell Transplantation Dose Alters Oligodendroglial and Neuronal Differentiation after Spinal Cord Injury

Katja M. Piltti,^{1,2,3,*} Gabriella M. Funes,^{1,4} Sabrina N. Avakian,^{1,4} Ara A. Salibian,¹ Kevin I. Huang,^{1,4} Krystal Carta,¹ Noriko Kamei,^{1,2} Lisa A. Flanagan,^{1,3,4,5,6} Edwin S. Monuki,^{1,3,7} Nobuko Uchida,⁸ Brian J. Cummings,^{1,2,3,4} and Aileen J. Anderson^{1,2,3,4}

¹Sue & Bill Gross Stem Cell Center, University of California Irvine, Irvine, CA 92697, USA

²Physical & Medical Rehabilitation

³Institute for Memory Impairments & Neurological Disorders

⁴Anatomy & Neurobiology

⁵Department of Biomedical Engineering

⁶Department of Neurology

⁷Department of Pathology and Laboratory Medicine

University of California Irvine, Irvine, CA 92697, USA

⁸BOCO Silicon Valley, ReGen Med Division, Palo Alto, CA 94303, USA

*Correspondence: kpiltti@uci.edu

<http://dx.doi.org/10.1016/j.stemcr.2017.04.009>

SUMMARY

Multipotent human central nervous system-derived neural stem cells transplanted at doses ranging from 10,000 (low) to 500,000 (very high) cells differentiated predominantly into the oligodendroglial lineage. However, while the number of engrafted cells increased linearly in relationship to increasing dose, the proportion of oligodendrocytic cells declined. Increasing dose resulted in a plateau of engraftment, enhanced neuronal differentiation, and increased distal migration caudal to the transplantation sites. Dose had no effect on terminal sensory recovery or open-field locomotor scores. However, total human cell number and decreased oligodendroglial proportion were correlated with hindlimb girdle coupling errors. Conversely, greater oligodendroglial proportion was correlated with increased Ab step pattern, decreased swing speed, and increased paw intensity, consistent with improved recovery. These data suggest that transplant dose, and/or target niche parameters can regulate donor cell engraftment, differentiation/maturation, and lineage-specific migration profiles.

INTRODUCTION

Transplanted multipotent human CNS-derived stem cells propagated as neurospheres (hCNS-SCns) respond differently to the intact versus injured spinal cord microenvironment, suggesting that terminal differentiation of human neural stem cells (hNSCs) is dependent on either injury-induced cues or availability of a cell lineage-specific target niche (Sontag et al., 2014). However, the capacity of the spinal cord injury (SCI) niche to provide cues for donor human cell engraftment and lineage-specific integration sites in relationship to transplantation dose is unclear.

Few studies have investigated the effect of unmodified human neural stem/precursor cell dose in CNS injury or disease models (Ostenfeld et al., 2000; Keirstead et al., 2005; Rossi et al., 2010; Darsalia et al., 2011), and none of these have investigated the effect of transplant dose on tri-lineage fate or utilized constitutively immunodeficient models, in which xenogeneic graft rejection is sufficiently suppressed to observe donor cell expansion. Accordingly, in this study we investigated the effect of hCNS-SCns transplant dose (10,000–500,000 cells) on human cell engraftment, death, differentiation, lineage-specific migration, and recovery of sensory and locomotor function at 16 weeks post transplantation (WPT) after SCI in immuno-

deficient non-obese diabetic (NOD)-severe combined immunodeficiency (SCID) mice.

RESULTS

Total Number of Human Cells and Long-Term Cell Proliferation in Each Dose Group

hCNS-SCns at cell doses of 10,000 (low), 100,000 (medium), 250,000 (high), or 500,000 (very high) were transplanted into the spinal cords of immunodeficient NOD-*scid* mice in the early chronic stage 30 days after moderate thoracic SCI, and histological parameters assessed 16 WPT (Figures 1A and S1). Unbiased stereological analysis of T6–T12 spinal cord segments revealed that the total number of donor human cells was significantly greater in the very-high- and high-dose groups in comparison with the low- or medium-dose groups (Figure 1B). A significant positive correlation was observed between transplant dose and number of human cells in the SCI microenvironment (Figure 1C), suggesting a linear relationship between these factors. However, there was a significant improvement in goodness of fit when a second-order polynomial was applied to the dataset containing all dose groups ($r^2 = 0.7$, $p \leq 0.02$ versus $r^2 = 0.6$, $p \leq 0.8$), which was not apparent

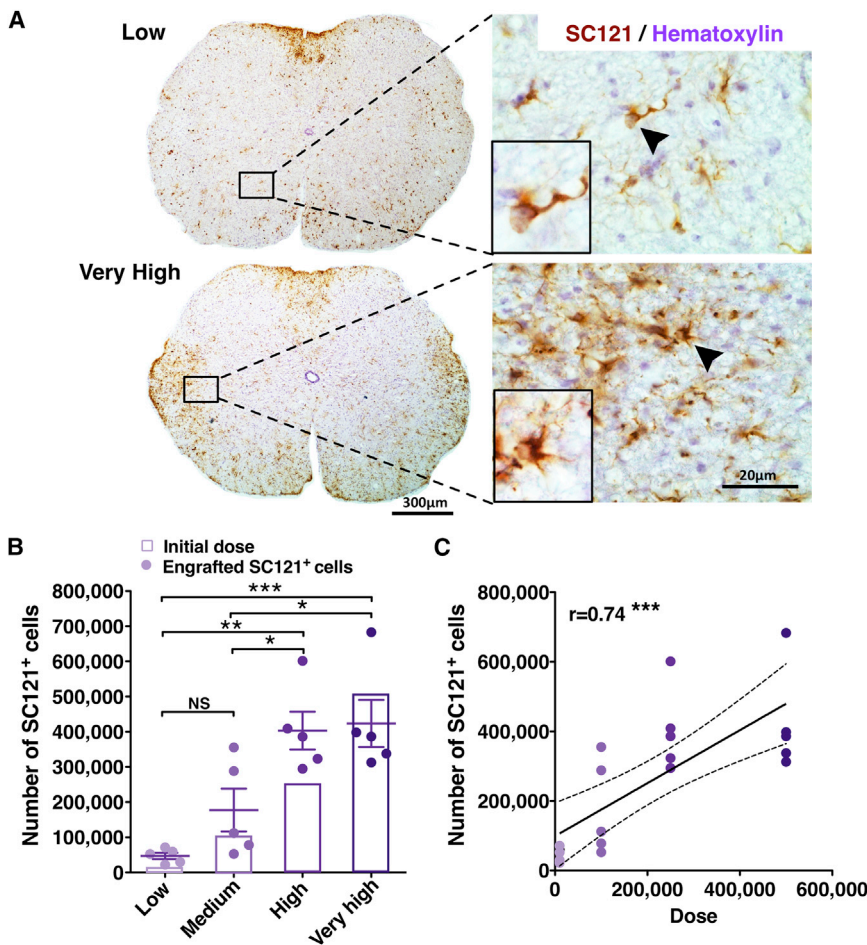


Figure 1. Transplantation of hCNS-SCNs in Early Chronic SCI, at 30 dpi, Results in a Linear Increase in Engraftment that Is Positively Correlated with Initial Transplantation Dose

(A) Representative coronal spinal cord sections immunostained for SC121 (STEM121) and hematoxylin 16 WPT. Arrowheads indicate the cells in the insets.

(B) Stereologically quantified SC121⁺ human cell number was significantly greater in high- and very-high-dose groups versus low- and medium-dose groups at 16 WPT. One-way ANOVA, $p = 0.0002$; Tukey's test, $*p \leq 0.05$, $**p \leq 0.001$, $***p \leq 0.0001$. NS, not significant. Colored dots, individual animals with mean \pm SEM; colored outlined bars, initial transplant dose.

(C) Correlation analysis revealed a significant positive relationship between greater transplant dose and SC121⁺ cell number (Pearson $r = 0.74$; $***p \leq 0.0001$). Colored dots, individual animals by dose group with regression line \pm SEM. All data $n = 5$ animals/group.

when the very-high-dose group was eliminated from the dataset; ($r^2 = 0.7$, $p \leq 1.0$), suggesting a plateau of donor cell engraftment at the highest (500,000 cells) transplant dose (Piltti et al., 2015). This change was not related to differences in either cell death, as assessed by cleaved CASP3, or proliferation, as assessed by SC121⁺/MKI67⁺ human cells, as no significant differences were observed in these measures between groups (Piltti et al., 2015).

Detailed histological analysis of human cells in spinal cord tissue showed no evidence of abnormal cellular morphology or mass formation in any dose group. However, 80% of the animals (4/5 mice) in the very-high-dose group and 40% of the animals (2/5 mice) in the high-dose group exhibited human cells or clusters of human cells that appeared to be localized within the central canal (Figure 2). No human cells were detected inside the central canal in the low- or medium-dose group animals, and chi-square analysis revealed a significantly greater probability for human cell entry into the central canal in the high- and very-high-dose groups (Figure 2). Ectopic ventricular donor human cell clusters from similar hNSC lines have been reported after transplantation into the brains of trans-

genic mice (Marsh et al., 2017). Evaluation of human cells by a clinical neuropathologist did not suggest gross changes in cell fate or proliferation phenotype when compared with the rest of the human cell population localized within the parenchyma. Critically, however, these data suggest that increasing transplantation dose may increase donor cell entry into the central canal, and the long-term effects of localization of these cells in a proliferative neuroepithelial environment are unknown.

Transplant Dose Alters the Proportion of Human Oligodendroglial and Neuronal Lineage Cells

hCNS-SCNs exhibited differentiation into all three neural cell lineages (Figures 3 and S2), as described previously (Salazar et al., 2010; Piltti et al., 2013a, 2013b). To assess the relationship between transplant dose and the phenotypic fate of engrafted donor human cells, we performed unbiased stereological quantification of human cells expressing tri-lineage markers. The total number of SC121⁺/OLIG2⁺ oligodendroglial lineage cells (Figures 3A and 3D), SC123⁺ astroglial lineage cells (Figures 3B and 3E), and SC121⁺/DCX⁺ neuronal lineage cells (Figures 3C and 3F) was

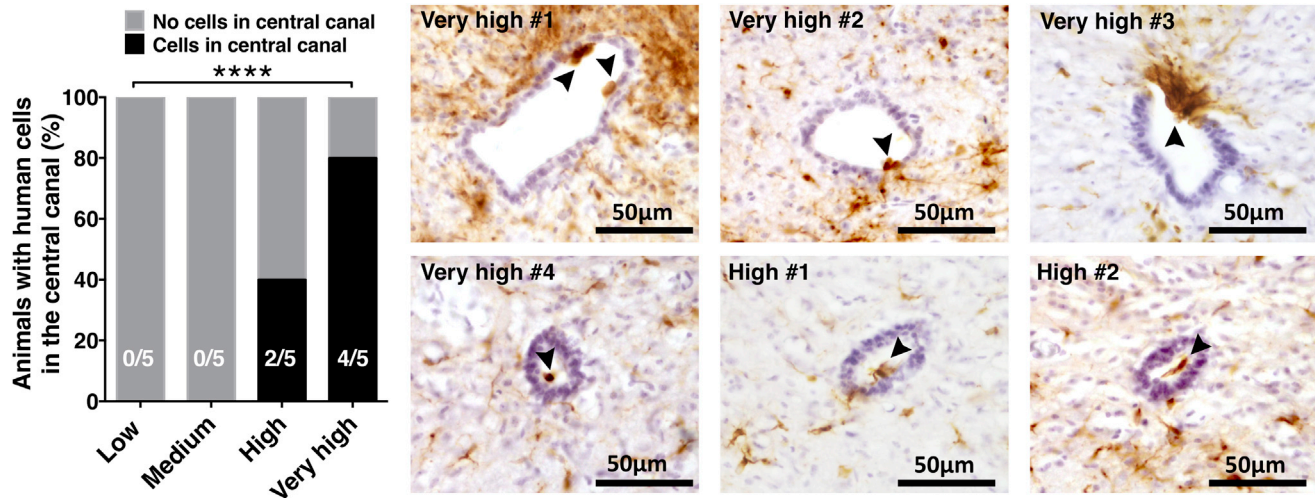


Figure 2. High and Very-High Transplantation Doses Increase Probability for Human Cell Entry into the Central Canal

Human cells or clusters of human cells were found within the central canal in 80% of the animals (4/5 mice) in the very-high-dose group and 40% of the animals (2/5 mice) in the high-dose group exhibited human cells (arrow heads) localized within the central canal. No human cells were detected inside the central canal in the low- or medium-dose group animals. Chi-square test revealed significantly greater probability for human cell entry into the central canal in the high- and very-high-dose groups ($****p \leq 0.0001$). Brown, SC121; purple, hematoxylin.

significantly greater in the very-high- and high-dose groups in comparison with the low- or low/medium-dose groups. In parallel, Pearson correlation analysis revealed a significant positive relationship between the total number of SC121⁺ human cells and each lineage-specific marker analyzed (Figures 3G–3I), suggesting a linear relationship between transplant dose and cell fate 16 WPT.

The effect of transplantation dose on the proportion of donor human cells exhibiting lineage-specific markers was analyzed by normalizing the total number of cells in each lineage to the total human cell number quantified in each animal. The proportion of SC121⁺/OLIG2⁺ cells was significantly greater in the low-dose group in comparison with the high- or very-high-dose groups (Figure 4A), and a significant negative correlation ($r = -0.63$) was observed between the number of SC121⁺ human cells and the proportion of human SC121⁺/OLIG2⁺ oligodendroglial cells (Figure 4B). In contrast, neither the proportion of SC123⁺ astrocytes nor the proportion of SC121⁺/DCX⁺ neuronal precursors exhibited significant differences between dose groups (Figures 4C and 4E), and no significant correlations were found between the total number of SC121⁺ human cells and proportional quantification of these markers (Figures 4D and 4F). Taken together, these data suggest that increasing transplant dose decreased the proportion of human cells differentiating along the oligodendroglial lineage in the SCI microenvironment, but did not affect the proportion of human cells differentiating into either the astroglial lineage or early neuronal lineage.

The sum of cell proportions positive for nuclear OLIG2, human GFAP, or DCX revealed that a fraction of cells had gone undetected by these markers. This fraction was as large as 21% in the very-high-dose group, with a significant difference between the low-dose group and the high- or very-high-dose groups (Figure S3A, one-way ANOVA $p = 0.03$, Student's two-tailed t test $*p \leq 0.05$). Further, a significant negative relationship was observed between the number of SC121⁺ human cells and the proportion of human cells expressing tri-lineage markers (Figure S3B, Pearson $r = -0.61$, $**p \leq 0.004$). We hypothesized that the unlabeled population of SC121⁺ human cells in the high- and very-high-dose groups could be due to a change in maturation of either oligodendroglial or neuronal lineage cells. We tested this possibility by immunostaining for more mature differentiation markers in the low- and very-high-dose groups, focusing on the oligodendroglial marker APC and the neuronal markers TUBB3 and RBFOX3. Stereological quantification of APC⁺/OLIG2⁺ human cells revealed no significant difference in the proportion of APC⁺ human oligodendrocytes between the low-dose group (1.2%) and the very-high-dose group (1.7%) (Figure 4G), suggesting that oligodendroglial maturation was not altered by transplantation dose. In contrast, quantification of human SC121⁺ cells expressing TUBB3 (Figures S2I–S2L) revealed a significant increase in the proportion of human neuronal lineage cells expressing this maturation marker between the low-dose group (1%) and the very-high-dose group (7%) (Figure 4G) at 16 WPT. Furthermore,

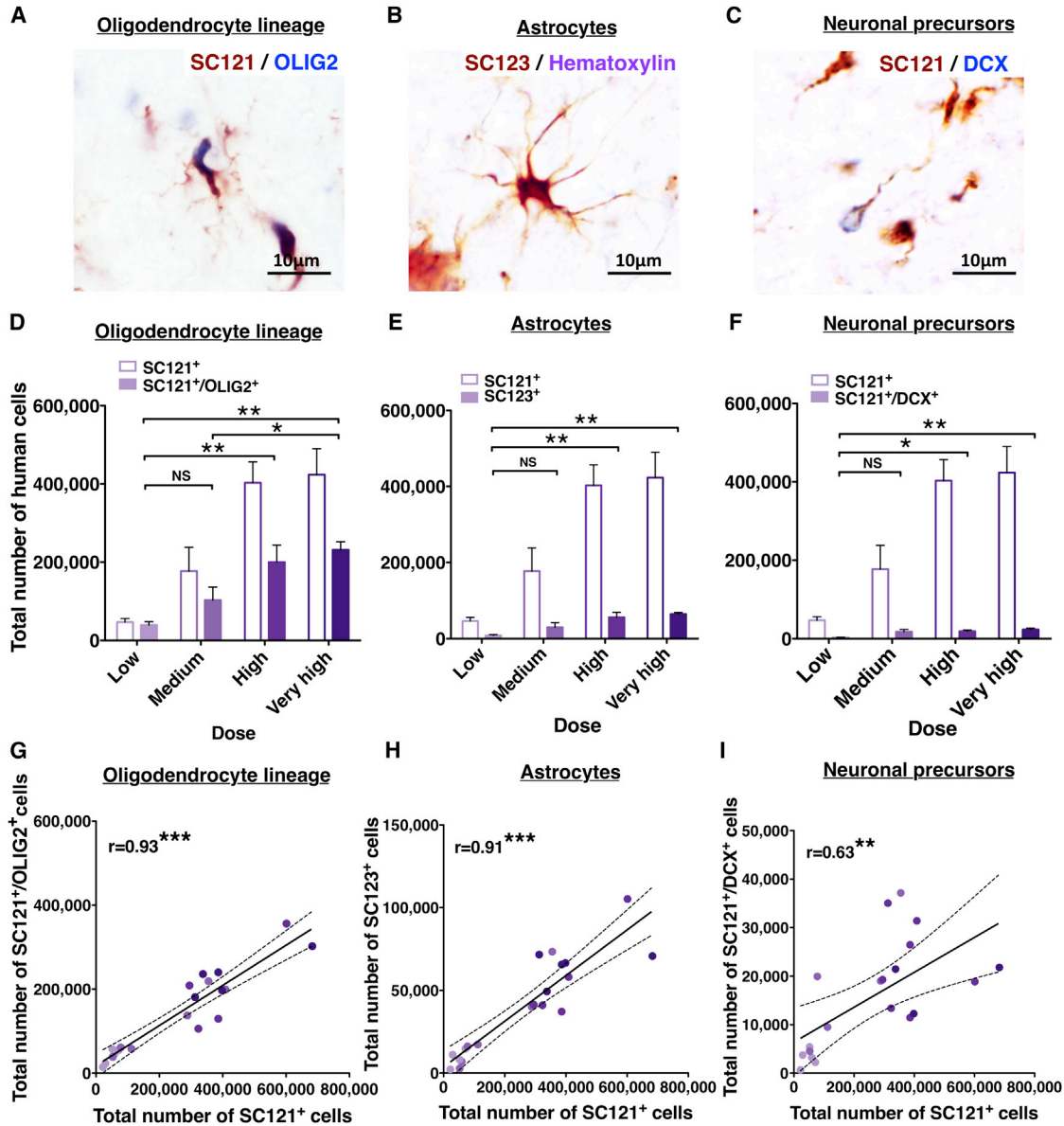


Figure 3. Relationship between Transplantation Dose and Phenotypic Fate Marker Expression by hCNS-SCNs at 16 WPT

(A–C) Representative images for (A) SC121⁺/OLIG2⁺ human oligodendroglial lineage cells, (B) SC123⁺ (STEM123)/hematoxylin⁺ human astrocytes, and (C) SC121⁺/DCX⁺ human neuronal lineage cells.

(D–F) Total numbers of stereologically quantified lineage specific cells were significantly greater in high- and very-high-dose versus lower-dose groups. Solid colored bars, total donor human lineage maker⁺ cells/group. Colored outlined bars, total SC121⁺ human cells/group, mean ± SEM. Total numbers of stereologically quantified lineage-specific cells were significantly greater in high- and very-high-dose versus lower-dose groups. One-way ANOVA, $p = 0.001$, $p = 0.002$, $p = 0.009$, respectively; Tukey's test * $p \leq 0.05$, ** $p \leq 0.001$. NS, not significant.

(G–I) Correlation analyses of total number of SC121⁺ human cells versus human lineage-specific cells (SC121⁺/OLIG2⁺, SC123⁺/hematoxylin, or SC121⁺/DCX⁺); Pearson $r = 0.93$, 0.91 , or 0.63 , respectively. *** $p \leq 0.0001$, ** $p \leq 0.003$. Colored dots, individual animals by dose group with regression line ± SEM. All data $n = 5$ animals/group.

SC121⁺ cells in the very-high-dose group were found to express the terminal neuronal differentiation marker RBFOX3; in contrast, SC121⁺/RBFOX3⁺ cells were never observed in the low-dose group (Figures 4H and 4I). Addi-

tion of quantification for APC⁺ and TUBB3⁺ human cells, therefore, increased the fraction of lineage committed cells in the very-high-dose group to be comparable with that in the low-dose group (Figure S3C). These data suggest that

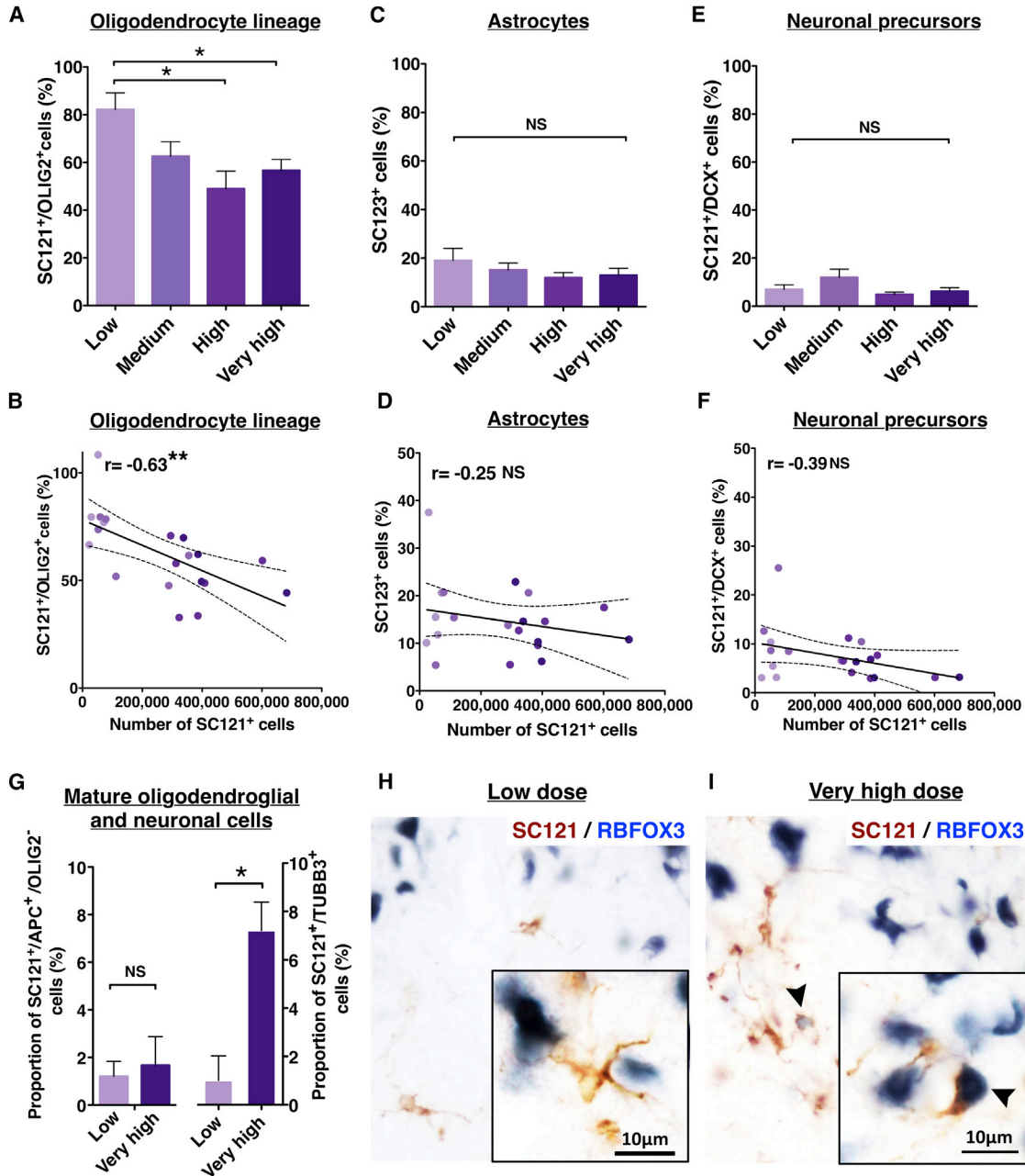


Figure 4. Transplantation Dose Affects hCNS-SCns Lineage Selection at 16 WPT

(A, C, and E) Proportion of human lineage-specific cells (SC121⁺/OLIG2⁺, SC123⁺/hematoxylin or SC121⁺/DCX⁺) by dose group. One-way ANOVA $p = 0.01$; Student's two-tailed t test $*p \leq 0.02$. NS, not significant.

(B, D, and F) Correlation between the total number of SC121⁺ human cells and the lineage-specific human cells; Pearson $r = -0.63$, $**p \leq 0.003$.

(G) Proportion of SC121⁺/OLIG2⁻/APC (CC-1)⁺ mature human oligodendrocytes and SC121⁺/TUBB3⁺ human neurons. Student's two-tailed t test $*p \leq 0.02$.

(H) SC121⁺ cells in the low-dose group were rarely positive for the terminal neuronal differentiation marker RBFOX3 (NEUN).

(I) In contrast, SC121⁺/RBFOX3⁺ cells (arrowhead) were often observed in the very-high-dose group.

(A), (C), (E), and (G), mean \pm SEM. (B), (D), and (F) colored dots, individual data points in each dose group with regression line \pm SEM. (A–F) $n = 5$ animals/group; (G) $n = 3$ animals/group.

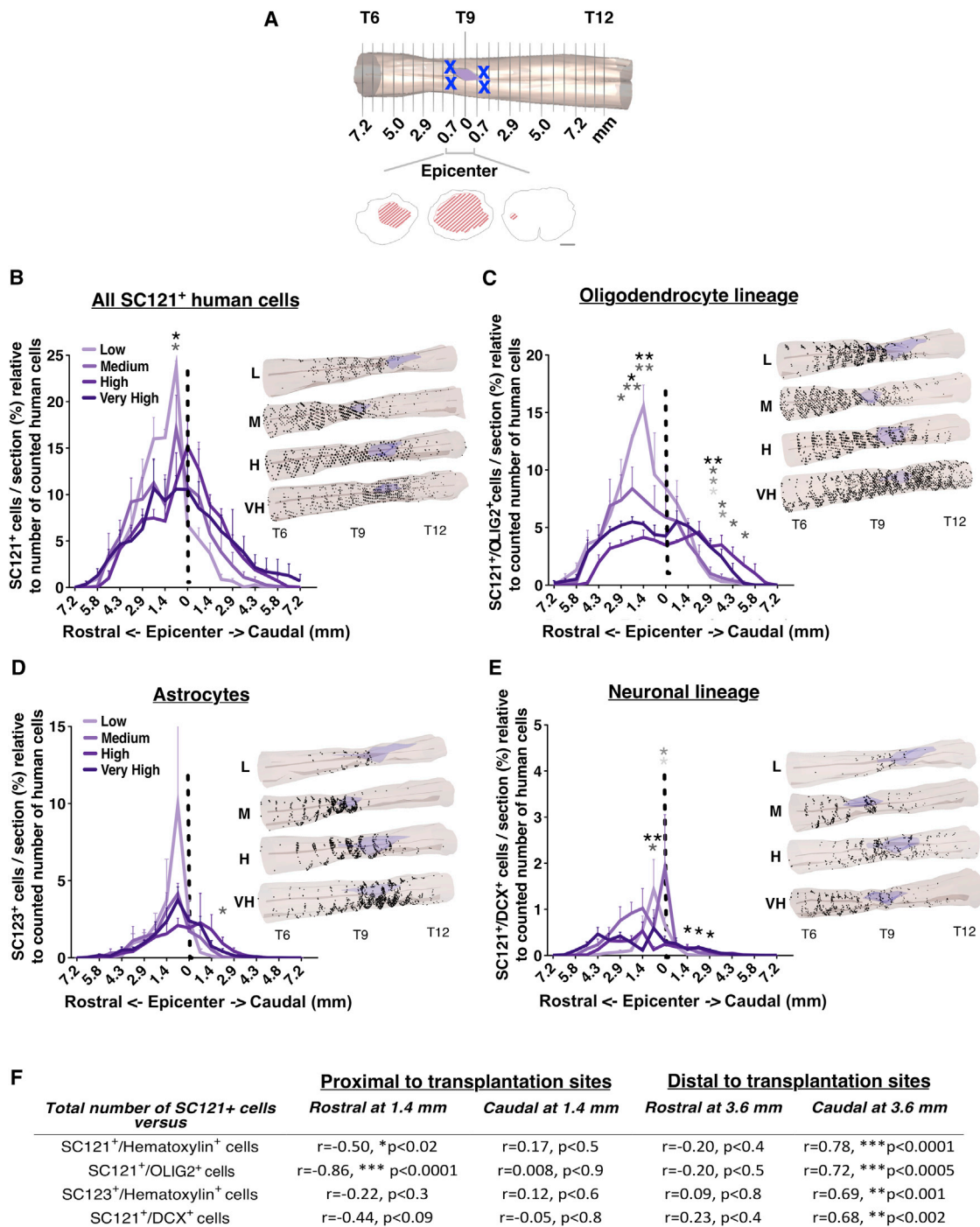


Figure 5. hCNS-SCns Migration as a Proportion of Engraftment

(A–E) Schematic dorsal view of the T6–T12 spinal cord segment illustrating the lesion epicenter (purple, reference location = 0), transplantation sites (x's), and analyzed coronal sections (0.72 mm apart; vertical lines). Positional migration data were plotted relative to the injury epicenter, identified as the coronal section with the largest cross-sectional lesion area (red hatched lines). Scale bar represents 300 μ m. Proportional localization for all SC121⁺ donor human cells (B), SC121⁺/OLIG2⁺ human cells (C), SC123⁺ human cells (D), and SC121⁺/DCX⁺ human cells (E) was calculated as the percentage of hCNS-SCns per section relative to the total number of counted human cells, mean \pm SEM. One-way ANOVA $p \leq 0.05$; Tukey's t test * $p \leq 0.05$, ** $p \leq 0.001$. Color coding for asterisks: black, low- versus very-high-dose; dark gray, low- versus high-dose; mid-gray, medium- versus very-high-dose; light gray, medium- versus high-dose. Insets in (B)–(E) show 3D reconstructions of hCNS-SCns distribution based on optical fractionator data in representative spinal cords selected from (legend continued on next page)



increasing transplant dose decreased the proportion of human oligodendroglial cells and increased the proportion of neuronal cells expressing mature lineage markers in the moderately injured spinal cord microenvironment.

hCNS-SCns Dose and Cell Lineage-Specific Migration, Proportional Localization, in the Injured Spinal Cords

To investigate the relationship between hCNS-SCns transplantation dose and human cell migration we aligned sections by location relative to the SCI epicenter, designated as the most damaged tissue section (Figure 5A), and plotted human cell distance from that 0 mm reference point. Analysis of total human cell number in each quantified section (Figure S4) revealed that hCNS-SCns in all dose groups exhibited extensive migration. Human cells were localized up to 7 mm rostral and caudal to the transplantation sites and injury epicenter, with no significant differences between groups (Figures 5 and S4; Piltti et al., 2015). However, the low-dose group exhibited a significantly greater proportion of total SC121⁺, OLIG2⁺ oligodendroglial, and DCX⁺ early neuronal human cells in the region rostral and proximal to the epicenter (Figures 5B–5E). In contrast, both the high- and very-high-dose groups shifted human cell localization to a more even distribution, and significantly increased proportions of human oligodendroglial, astroglial, and early neuronal cells in the caudal parenchyma distal to the injury epicenter (Figures 5B–5E). In parallel, correlation analysis using designated reference points revealed a negative relationship between the total number of engrafted cells and the proportion of rostrally located SC121⁺ cells or oligodendroglial lineage proximal to the epicenter (Figure 5F). In addition, there was a linear relationship between increasing dose and proportion of caudally located human cells distal to the epicenter (Figure 5F). These changes in donor cell distribution between the low- and very-high-transplantation doses could reflect the retention of donor cells in target areas for remyelination and axonal sprouting.

Dose-Dependent versus Microenvironmental Changes in hCNS-SCns Gene Expression

Target niche and transplantation cell dose could interact to alter donor human cell engraftment, migration, and lineage selection. To investigate the mechanisms underlying dose-dependent versus microenvironment-related human cell differentiation and migration, we constructed a paradigm in which we could separate the relative contributions

of each of these factors. First, we compared gene expression profiles of human cells transplanted into the early chronic SCI microenvironment at the low-versus the very-high-dose and re-isolated at 2 WPT, factoring for the relative contribution of dose (Paradigm 1). Second, we compared gene expression of very-high-dose human cells injected into in a 3D fibrin matrix (Figure S5) and differentiated for 2 weeks in vitro versus transplanted in vivo and re-isolated at 2 WPT, factoring for the relative contribution of microenvironment (Paradigm 2). The rheological properties of this matrix are comparable with those of brain and spinal cord (Arulmoli et al., 2016), making an in vitro 3D culture microenvironment in which cells can undergo injection using an identical paradigm to that employed in vivo, while removing the microenvironmental effects contributed by cell-cell contacts between mouse host and donor human cells, as well as the host innate immune response to injection. To enable specific re-isolation of human cells after in vivo transplantation for these experiments, we generated a hCNS-SCns line expressing AAVS1 safe-harbor targeted EGFP reporter driven by a CAGG promoter, which is constitutively active in both stem cells and their differentiated progeny (Liew et al., 2007). hCNS-SCns-CAGG-eGFP were transplanted into the early chronic 30 days post SCI microenvironment and retrieved using fluorescence-activated cell sorting (FACS). Gene expression comparisons were conducted using RT2 Human Neurogenesis Profiler Array real-time PCR analysis, which contains 84 target genes related to the processes of human neurogenesis, neural stem cell differentiation, proliferation, and migration. The target gene list includes growth factors, cytokines, and transcription factors related to differentiation, synaptic function, apoptosis, and cell adhesion. A ≥ 1.5 fold-change and $p \leq 0.1$ was used as a cutoff for differential gene expression. Gene lists ranked based on fold-change and a p value demonstrate good reproducibility across multiple microarrays and PCR arrays (Shi et al., 2006, 2010).

Array analysis revealed five differentially expressed genes in human cells from the very-high-dose in vivo condition compared with the low-dose condition (Figure 6A); of these, differential expression of three genes, *ARTN*, *MAP2*, and *NRP* was observed only in Paradigm 1 and hypothesized to be specifically dose related (Figure 6C). In parallel, array analysis revealed 38 differentially expressed genes in the very-high-dose in vivo condition compared

each dose group/cell lineage; the spinal cord with cell numbers closest to the group mean was selected for illustration. Dark purple dots, human cells; purple shading, epicenter. Sampling sequence 1/24 with parameters specific to each lineage marker (Table S1B); dose groups are therefore comparable within but not between markers.

(F) Pearson's correlation analyses were performed using reference points either proximal to cell transplantation sites (1.4 mm rostral/caudal), or distal to cell transplantation sites (3.6 mm rostral/caudal; halfway between the epicenter and maximal migration distance of 7 mm). All data $n = 5$ animals/group.

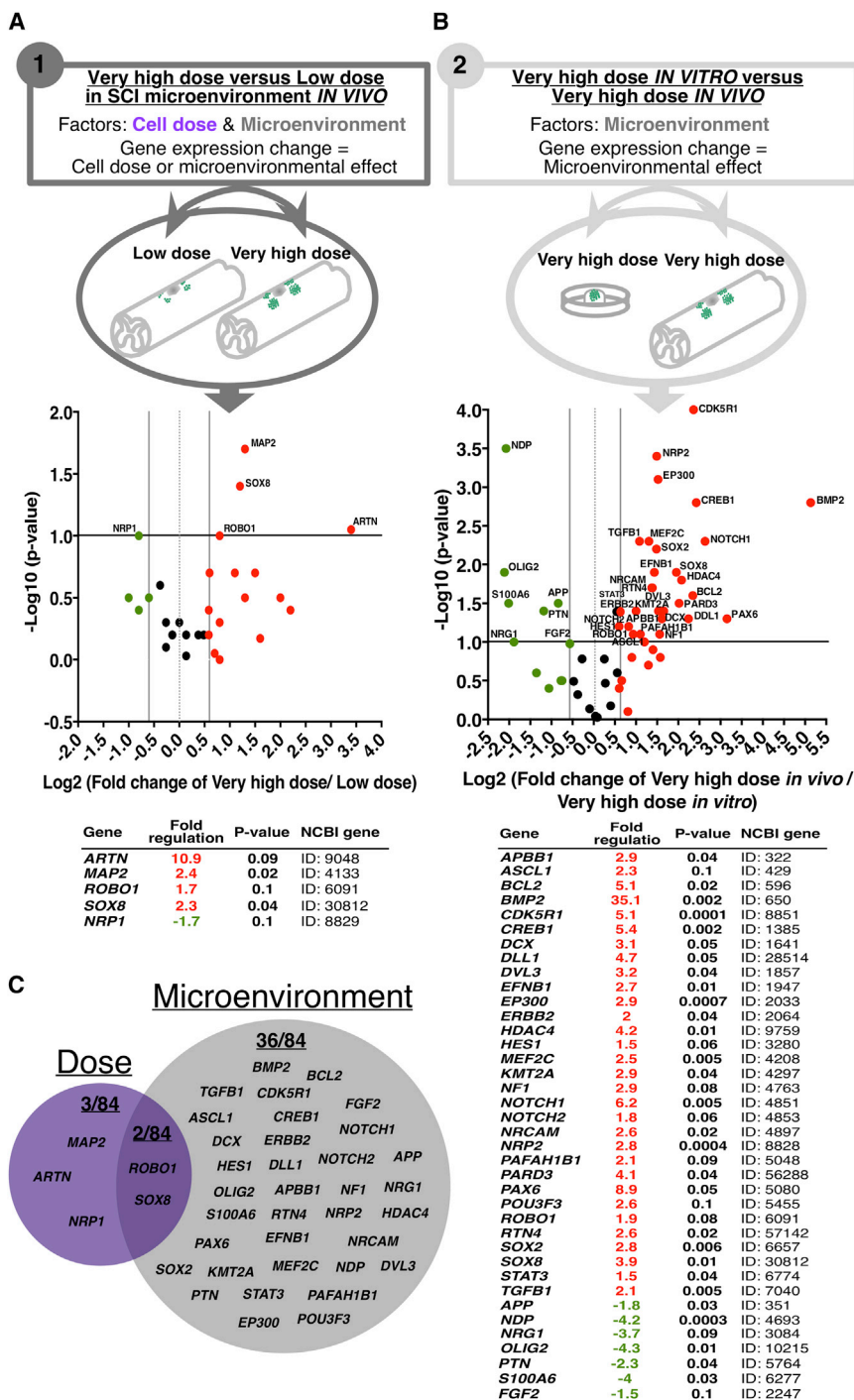


Figure 6. Dose-Dependent versus Microenvironmental Gene Expression Changes Analyzed Using RT2 Human Neurogenesis Profiler Array Real-Time PCR Analysis

(A) Paradigm 1: gene expression of human cells transplanted into the early chronic SCI microenvironment at low- versus very-high-dose and re-isolated at 2 WPT, factoring for the relative contribution of dose.

(B) Paradigm 2: gene expression of very-high-dose human cells injected into in a 3D fibrin matrix and differentiated for 2 weeks in vitro versus transplanted in vivo and re-isolated at 2 WPT, factoring for the relative contribution of microenvironment. Differential expression cutoff at ≥ 1.5 fold-change and $p \leq 0.1$. Upregulated (red) and downregulated (green) genes are shown as a volcano plot and table with corresponding fold changes and p values.

(C) Venn diagram of differentially expressed dose-regulated (3/84), microenvironment-regulated (36/84), and co-regulated (2/84) genes. $n = 3$ individual experiments/paradigm.

with the 3D matrix in vitro condition (Figure 6B); of these, differential expression of 36 genes was observed only in Paradigm 2 and hypothesized to be specifically microenvironment related (Figure 6C). Raw Ct values under Table S2. These data suggest that both injury microenvironment and transplantation dose contribute to human cell responses.

Effect of hCNS-SCns Transplantation Dose and Cell Phenotype on Recovery of Sensory and Locomotor Function

To assess the relationship between transplantation dose and sensory recovery/development of hyperalgesia, we conducted Hargreaves hyperalgesia testing at pre-transplantation baseline and at 13 WPT. In concordance with

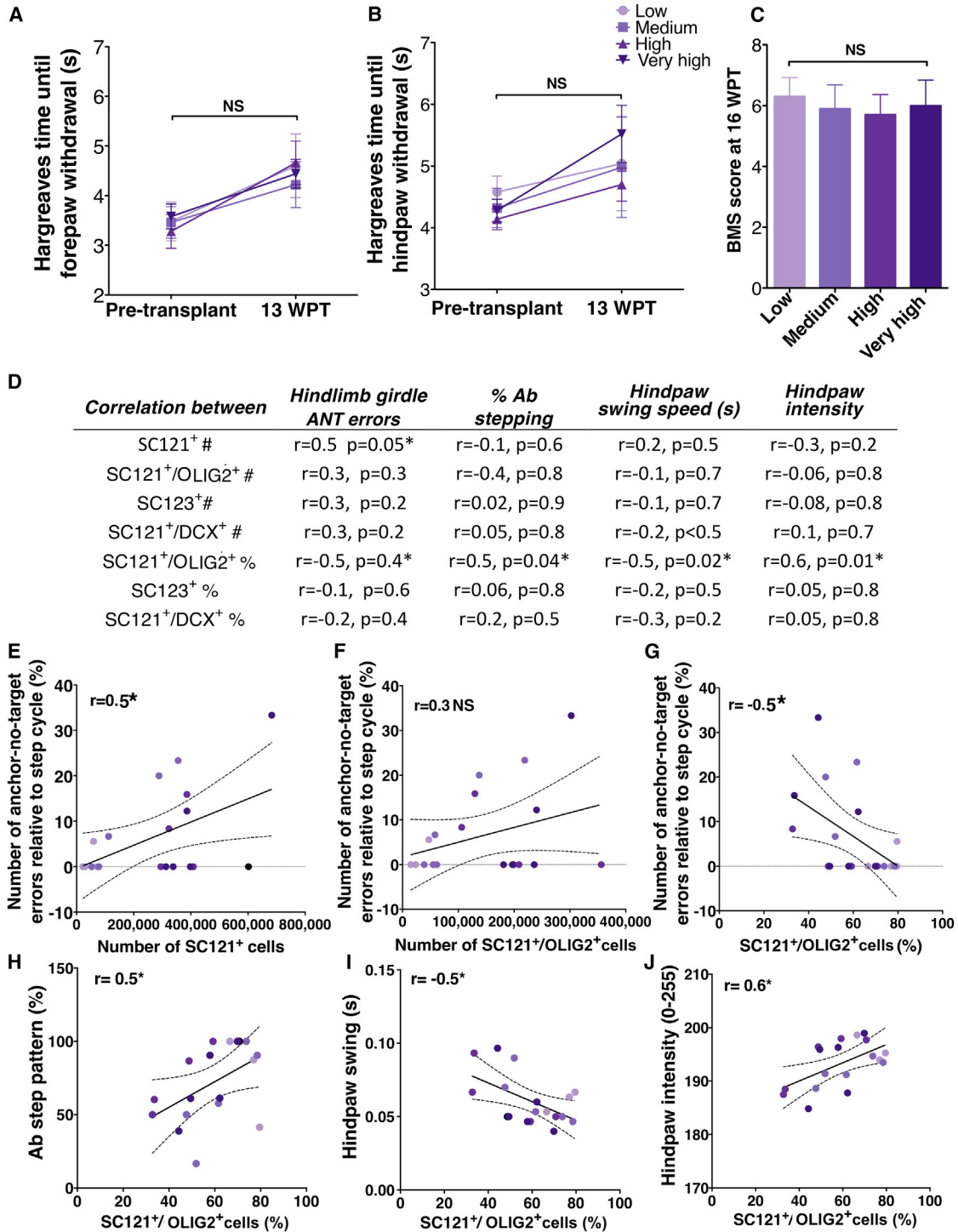


Figure 7. Effect of hCNS-SCNs Transplantation Dose and Cell Phenotype on Recovery of Sensory and Locomotor Function

(A and B) Hargreaves hyperalgesia testing prior to transplantation and at 13 WPT revealed no significant interaction between the number of forepaw or hindpaw withdrawals in the dose groups over time (two-way ANOVA $p = 0.62$ and $p = 0.9$, respectively), or significant differences between dose groups either pre-transplantation or 13 WPT (Bonferroni post hoc test, $p > 0.05$). Mean \pm SEM; $n = 5$ animals/group. NS, not significant.

(C) Open-field locomotor performance showed no significant differences between groups at 16 WPT (one-way ANOVA $p = 0.98$). Mean \pm SEM; $n = 5$ animals/group.

(legend continued on next page)

our previous transplantation studies using a single donor human cell dose (Piltti et al., 2013a, 2013b), no significant interaction was found between the number of forepaw or hindpaw withdrawals in the dose groups over time (Figures 7A and 7B, two-way ANOVA $p = 0.62$ and $p = 0.9$, respectively). In addition, no significant differences were found between dose groups either pre-transplantation or at 13 WPT (Figures 7A and 7B, Bonferroni post hoc test, $p > 0.05$), suggesting no relationship between transplant dose and sensory recovery/development of hyperalgesia.

To investigate the general relationship between transplant dose and locomotor recovery, we conducted terminal open-field testing and CatWalk gait analysis. Mice in all dose groups recovered to frequent-consistent stepping with varying coordination (BMS scale of 5 and above), with no significant difference between groups at 16 WPT at the Ns employed in this study (Figure 7C, one-way ANOVA $p = 0.98$). Because assessment of coordination is relatively limited using open-field locomotor assessments, we focused CatWalk gait analysis on parameters related to this aspect of hindlimb alternation and recovery using time relationships (phase lags, couplings) between girdle paws (specifically left and right hindlimb in our case), a sensitive, speed-independent measure of coordination (Hamers et al., 2006; Koopmans et al., 2006). Correlation analysis revealed a linear relationship between anchor-no-target (ANT) errors in hindlimb girdle couplings and the total number of engrafted SC121⁺ human cells (Figures 7D and 7E). These data suggest that increasing transplant dose had no overall effect on open-field locomotor recovery, but may have been associated with a negative impact on coordination.

Next we investigated the relationship between total human cell number for each lineage and ANT errors in hindlimb girdle couplings (Figures 7D and 7F); no significant differences were found. However, as described above, the dose-dependent increase in human cell number was associated with a decrease in proportion of SC121⁺/OLIG2⁺ cells; we therefore also analyzed the relationship between SC121⁺/OLIG2⁺ proportion and ANT errors, which exhibited a significant negative correlation (Figure 7G). In accordance, a positive correlation was observed between SC121⁺/OLIG2⁺ proportion and percentage Ab step pattern (Figures 7D and 7H), the most frequent step pattern observed before SCI. In parallel, a significant relationship was detected between the proportion of SC121⁺/OLIG2⁺ cells and hindlimb swing speed (Figures 7D and 7I) or hindpaw intensity (Figures 7D and 7J), both of which

have been associated with improved locomotor recovery post-SCI (Hamers et al., 2001). No correlations were detected between the proportion of human astroglial (SC123⁺) or neuronal (SC121⁺/DCX⁺) cells and the proportion of Ab step pattern, hindlimb swing speed, or hindpaw intensity (Figure 7D). Overall, these data suggest that the proportional ratio of oligodendroglial cells within the transplanted cell population, which was greatest in the lowest-dose group, may be more important for locomotor recovery than increasing the total number of engrafted human cells.

DISCUSSION

The effect of transplantation dose on donor cell engraftment and lineage-specific integration has been characterized only in hematopoietic stem cells, where the magnitude of donor cell engraftment and mobilization is positively correlated to transplant dose (Chen et al., 2004; Liu et al., 2010). Despite the paucity of studies in other tissues, it has generally been assumed that “more is better” in the context of donor cell transplantation studies. However, target niche and transplantation dose could interact to alter lineage selection. The results of the few previous studies investigating the effect of unmodified hNSC/precursor dose in CNS injury or disease models have been mixed with respect to impact on engraftment (Ostenfeld et al., 2000; Darsalia et al., 2011). Critically, however, these studies were performed in pharmacologically immunosuppressed xenotransplantation models, in which the lack of adequate immunosuppression could lead to a dose-dependent increase in immune rejection, confounding interpretation of these relationships. The current data, which utilized constitutively immunodeficient models, may thus permit a more precise analysis of niche dynamics.

Characterization of the effect of increasing transplantation dose (10,000–500,000 cells) revealed a linear relationship between cell dose and the total number of engrafted cells, suggesting that human cell engraftment was scalable within the SCI niche. However, increasing cell dose negatively affected human cell proliferation and expansion at the very-high-transplant dose (500,000 cells) (Piltti et al., 2015), suggesting that the SCI niche may have a limit for accommodating donor cells. In addition, increasing cell dose strongly correlated with localization of human cells inside the central canal, suggesting dose-related donor cell entry into the central canal adjacent to the lesion.

(D–J) Correlation analyses of CatWalk gait parameters (ANT errors in hindlimb girdle [RH-LH] couplings, percentage Ab step pattern, hindlimb swing speed, and hindpaw intensity) versus donor human cell engraftment (total SC121⁺ number [#] and proportional fate [%] quantification) at 16 WPT. * $p \leq 0.05$; colored dots, individual data points in each dose group with regression line \pm SEM; $n = 3$ –5 animals/group.



Parallel investigation of the relationship between transplantation dose and lineage selection revealed a positive linear relationship between the total number of engrafted human cells and the number of human cells exhibiting lineage-specific differentiation markers (OLIG2, GFAP, or DCX). In addition, in accordance with our previous studies, the majority of hCNS-SCNs adopted an oligodendroglial fate, irrespective of transplant dose. However, proportional analysis revealed a surprising dose effect on early oligodendroglial differentiation and migration, in which the low-dose group exhibited a significantly greater proportion of donor OLIG2⁺ cells. This type of effect has not been previously reported in the diseased or injured CNS niche, but several *in vitro* and *in vivo* studies have suggested that differentiation of oligoprogenitors is controlled by biophysical interactions and cell density-dependent feedback inhibition (Nakatsuji and Miller, 2001; Bershada et al., 2008; Rosenberg et al., 2008; Hughes et al., 2013). These data were paralleled by a dose-dependent increase in differentiation to mature neurons.

In this regard, an additional variable that could be critical to donor cell lineage selection is migration within the niche. Although increasing cell dose increased human cell migration in the early post-transplantation period, this effect was transient, as no changes were detected in long-term maximal rostral-caudal migration (Piltti et al., 2015). Importantly, however, the low-dose group exhibited a significantly greater proportional localization of human cells, including oligodendroglial and early neuronal lineage cells, in the rostral region proximal to the injury epicenter. In contrast, increasing cell dose increased caudal migration of human cells and shifted proportional cell localization to a more even distribution throughout the entire T6–T12 segment. In this regard, oligodendroglial cell death after SCI has been reported to be greatest rostral to the epicenter, and to continue into the chronic stages post-injury (Shuman et al., 1997; Warden et al., 2001). Taken together, these data suggest a dynamic response of transplanted hNSC to the injured niche. One possibility is that the available targets driving oligodendroglial lineage selection proximal to the injury epicenter can become filled by transplanted cells in a dose-dependent manner, resulting in an increase in migration and proportional differentiation with increasing dose. In addition, the low-dose group may have re-directed tri-lineage differentiation based on local cues to “fill” the oligodendroglia depleted niche near the injection sites.

Although several studies have characterized microenvironment-dependent properties of transplanted mouse NSC in CNS injury models (Capone et al., 2007; Kumamaru et al., 2012), the dynamic interaction between transplant dose and human lineage selection in the injury/disease niche has not been well studied in any model system.

In our experimental paradigm, we probed the possibility to distinguish effects of transplant dose from that of the microenvironment on neurogenesis-related genes in transplanted hNSCs using real-time PCR analysis. Our *in vivo* differential gene expression comparison between hCNS-SCNs transplanted at low-dose and very-high-dose is based on a single time point of assessment, at 2 WPT. Although these data reflect a temporally narrow approach focusing on a limited number of genes, we found a small subset of genes that were differentially expressed in human cells specifically in association with changes in dose. In comparison with low-dose, very-high-dose human cells exhibited upregulation of microtubule-associated protein *MAP2* and neurotrophic factor *ARTN*, and downregulation of *NRP1*, which play roles in neuronal morphogenesis, migration, and support (Baloh et al., 1998; Teng et al., 2001; Schwarz and Ruhrberg, 2010). The gene expression changes in hCNS-SCNs transplanted at very-high-dose align with the histological analysis, where increased neural differentiation at 16 WPT was observed, supporting both approach feasibility and future analyses evaluating multiple timepoints and whole-transcriptome sequencing.

Analysis of the differentially expressed genes between the very-high-dose hCNS-SCNs *in vivo* and *in vitro* revealed a larger subset of genes associated with changes in the microenvironment. Differentially expressed genes in the *in vivo* transplanted hCNS-SCNs divided roughly into two categories: (1) cell survival and differentiation, and (2) neurite outgrowth and migration. Under the cell survival and differentiation category, *TGFβ*, *NOTCH*, and *BCL2* were robustly upregulated. *Tgfb1* upregulation in transplanted mouse neural cells in injured CNS has been reported to reflect a response to inflammatory activity, and both *Bcl2* and *Notch* increase NSC survival (Capone et al., 2007; Kumamaru et al., 2012; Koch et al., 2013). In parallel, observed changes in *BMP2*, *NOTCH*, *OLIG2*, *FGF2*, *ASCL1*, *DLL1*, and *PAX6* are consistent with previous reports of modulation of NSC differentiation and lineage selection (Zhou and Anderson, 2002; Wu et al., 2003; Cheng et al., 2007; Sugimori et al., 2007; Kumamaru et al., 2012; Koch et al., 2013; Vasconcelos and Castro, 2014; Li and Leung, 2015). For the neurite outgrowth and migration category, upregulation of genes such as *DCX* (Schaar et al., 2004), *NRP2* (Schwarz and Ruhrberg, 2010), and *EFNB1* (Tanaka et al., 2004) suggest increases in neuronal migration, axonal outgrowth, and guidance signaling. Finally, two differentially expressed genes exhibited parallel upregulation in the both dose versus microenvironment comparisons, *SOX8* and *ROBO1*, which are associated with spinal cord maturation (Cheng et al., 2001) and axon guidance, migration, or proliferation (Andrews et al., 2006; Borrell et al., 2012), respectively, suggesting that



both transplantation dose and injury microenvironment contribute to human cell responses post transplantation.

While there are several *in vitro* models for studying the biomechanics of neural tissue (Morrison et al., 2011), to our knowledge, no previous studies have attempted a direct comparison of gene expression between *in vivo* transplanted and *in vitro* cultured cells to investigate dose-dependent versus microenvironmental changes in gene expression. *In vitro* 3D models are useful to study neurobiological phenomena that are difficult to manipulate or measure *in vivo*, enabling isolation from host-donor cell interactions and host immune responses. However, it is important to recognize that these models generally lack tissue cytoarchitecture and a perfused vasculature, relying on passive diffusion for nutrients and waste disposal, which may limit interpretation.

No dose-related changes in open-field locomotor performance were reported by either Keirstead et al. (2005) (250,000 versus 1,500,000 human oligoprogenitor cells) or Iwai et al. (2014) (250,000 versus 1,000,000 mouse NSC). However, dose-related changes in recovery of coordination may be subtle and require more defined measures, e.g., kinematic analysis using CatWalk or other higher-order tasks. Consistent with this possibility, we detected a significant relationship between increasing proportion of human oligodendroglial cells and gait measures, such as percentage Ab step pattern, hindlimb swing speed, and hindpaw intensity, associated with improved locomotor recovery post SCI (Anderson et al., 2017). However, we also report that increasing transplant dose, which paralleled decreasing oligodendroglial lineage proportion, were both associated with an increase in coordination errors. Although speculative, one interpretation of these data would be that increased generation and integration of transplanted cells as mature neurons in the higher-dose groups could negatively modulate spinal circuitry without training or other intervention (Garcia-Alias et al., 2009; Maier et al., 2009; Garcia-Alias and Fawcett, 2012). This work, together with our previous data (Piltti et al., 2015), indicates that it is important to consider potential dose effects on donor cell engraftment, differentiation/maturation, lineage-specific migration, and locomotor recovery in the development of clinical cell transplantation protocols.

EXPERIMENTAL PROCEDURES

hNSC

Multipotent human fetal brain-derived neural stem cells (hCNS-SCns) were provided by STEMCELL (passage ≤ 12), as described previously (Cummings et al., 2005, 2009; Salazar et al., 2010; Piltti et al., 2013a, 2013b, 2015; Sontag et al., 2013; Anderson et al., 2017).

Contusion Injuries and Cell Transplantation

All experiments were conducted following the guidelines issued by UC Irvine's Institutional Animal Care and Use Committee. Bilateral 50-kDa contusion injuries and cell transplantations were performed as described by Piltti et al. (2015). In brief, female NOD-SCID mice (Jackson Laboratory) received a total of 10,000 (low dose), 100,000 (medium dose), 250,000 (high dose), or 500,000 (very high dose) cells as four 1.25 μ L injections (for a total of 5 μ L) into intact parenchyma adjacent to the lesion at early chronic stage 30 days post SCI. All animals received the same injection volume irrespective of dose group.

Behavioral Assessments

Assessment of recovery for sensory behavior/development of thermal hyperalgesia was conducted using Hargreaves testing (Hargreaves et al., 1988) pre-transplant (baseline) and at 13 WPT as described by Piltti et al. (2013a). Terminal locomotor recovery testing was conducted using BMS open-field test at 16 WPT (Basso et al., 2006) and CatWalk gait analysis at 15 WPT (Hamers et al., 2006). The number of ANT errors in hindlimb girdle couplings were normalized to total number of step cycles (right forepaw - right hindpaw - left forepaw - left hindpaw) in each crossing.

Randomization, Exclusion Criteria, and Group Numbers

Randomization, exclusion criteria, and blinding for histological analysis were conducted as described previously (Salazar et al., 2010; Piltti et al., 2015). In brief, pre-hoc exclusion criteria for stereological or behavioral assessments were unilateral bruising or abnormal force/displacement curves after contusion injury, or documentation of poor transplantation injection. All groups were conducted in parallel, and animal care, behavioral analyses, and histological analyses were performed by researchers blinded to experimental groups. Exclusions, and final group numbers used in histological or behavioral analysis are listed in Figure S1.

Tissue Collection, Sectioning, Immunohistochemistry, and Stereological Analysis

Tissue collection at 16 WPT, sectioning and immunohistochemistry were performed as described by Piltti et al. (2015). Antibodies and dilutions used are listed in Table S1A.

Stereological Analysis

Unbiased stereology was conducted using systematic random sampling, an optical fractionator probe, and Stereo Investigator version 9 (MicroBrightField). Parameters for the analysis are listed in Table S1B.

Cell Migration Analysis

Migration of human cells was determined using stereological data, and shown as the total number of human cells counted per section, and as the percentage of human cells per section relative to the total number of counted human cells.



Isolation of hCNS-SCNs from Injured Mouse Spinal Cord Using FACS

EGFP reporter under the hybrid promoter with human cytomegalovirus early enhancer and enhancer elements of chicken β -actin and rabbit β -globin (pCAGG) (Liew et al., 2007) was targeted into AAVS1 safe-harbor locus of hCNS-SCNs using the CompoZr Zinc Finger Nuclease (Sigma-Aldrich) and Amaxa Nucleofector electroporation (Lonza). Positive clones with stable EGFP expression were selected using 500 ng/mL of puromycin supplemented in the culture medium as described previously (Liew et al., 2007). Transplantation of eGFP-expressing human cells at low dose or very high dose were performed as described in the Contusion Injuries and Cell Transplantation sections. At 2 WPT, mice were anesthetized, transcardially perfused with PBS, and 5 mm segments of T9 dissected and dissociated using 0.5 mg/mL trypsin (Gibco) and 1 mg/mL collagenase (Sigma) for 20 min at 37°C. Cells were stained with propidium iodide (Thermo Fisher Scientific) and live eGFP-expressing human cells were separated using fluorescence-activated cell sorting (FACS Aria II, BD Biosciences) for isolation of total RNA. Each individual experiment consists of an average of 900 human cells pooled together from 2 to 5 low-dose group animals, or an average of 6,000 human cells from 1 to 3 very-high-dose group animals.

hCNS-SCNs Differentiation in 3D Salmon Fibrin Gels

Salmon fibrinogen (5 mg) and salmon thrombin (0.2 U) (Sea Run Holdings) were mixed with X-Vivo-based differentiation medium and polymerized into 50 μ L gels as described previously (Arulmoli et al., 2016). Similar to in vivo transplantations, eGFP-expressing human cells were injected into 3D fibrin gels (1.25 μ L per gel) at very high dose using a Nanoinjector and glass injection tips (see Supplemental Experimental Procedures for details). The number of cells per gel corresponds to the number of cells in a single in vivo injection site. After 2 weeks of in vitro differentiation, fibrin gels with hCNS-SCNs were collected for isolation of total RNA. Each individual experiment consists of total RNA pooled from the cells in two fibrin gels.

RNA Isolation, cDNA Synthesis, and Gene Expression Analysis by Real-Time PCR

Total mRNA from either FACS sorted or fish fibrinogen-grown NSC was isolated using a RNeasy Micro Kt (QIAGEN) and analyzed using an Agilent 2100 Bioanalyzer Pico Chip Kit. For each experiment, 1 ng of RNA was reverse transcribed using a Human Neurogenesis RT2 Profiler PCR Array-specific PreAMP cDNA Synthesis Kit and PreAMP Pathway Primer Mix (QIAGEN), according to the manufacturer's protocol. Relative quantification of gene expression in three individual experiments per group in each paradigm for the 84 gene targets present in the array was done using an RT2 Profiler PCR Array Data Analysis v.3.5 (QIAGEN), which calculates fold changes based on the $\Delta\Delta$ Ct method and p values using a Student's t test based on the triplicate $2^{(-\Delta\text{CT})}$ values for each gene in the group of interest compared with the control group. All datasets were normalized to geometric mean of *ACTB* and *GAPDH*.

Statistical Analysis

All data are shown as means \pm SEM. Statistical analysis were performed using Prism5 software, version 5.0 (GraphPad) using either

Pearson correlation coefficient, one-way ANOVA combined with Tukey's post hoc t test or Student's two-tailed t test, or two-way ANOVA combined with Bonferroni post hoc test. $p \leq 0.05$ was considered to be statistically significant.

SUPPLEMENTAL INFORMATION

Supplemental Information includes Supplemental Experimental Procedures, five figures, and two tables and can be found with this article online at <http://dx.doi.org/10.1016/j.stemcr.2017.04.009>.

AUTHOR CONTRIBUTIONS

Conception and Design, and/or Assembly of Data, Data Analysis, and Interpretation, Manuscript Writing, K.M.P.; Collection and/or Assembly of Data, G.M.F., S.N.A., A.A.S., K.I.H., and K.C.; Provision of Study Material, N.U., N.K., and L.A.F.; Neuropathological Evaluation of Histological Sections, E.S.M.; Conception and Design, Financial Support, Manuscript Writing, and Final Approval of Manuscript, B.J.C. and A.J.A.

ACKNOWLEDGMENTS

We want to thank technical staff at the Christopher and Dana Reeve Foundation Core (CDRF core), especially Rebecca Nishi, M.S., Hongli-Liu, M.D., Chelsea Pagan, Christina de Armond, and Elizabeth Hoffman, for their help with animal surgeries. We also thank Janahan Arulmoli, Ph.D., Eileen Do, Colleen Worne, and Antoinette Hu for technical assistance. This study was supported in part by NIH (Grant R01-NS049885) to A.J.A. and B.J.C.; Christopher Reeve Foundation (AAC-2005) to A.J.A.; and by CIRM Postdoctoral Training Grant (TG2-01152) to K.M.P.

Received: October 15, 2014

Revised: April 7, 2017

Accepted: April 7, 2017

Published: May 4, 2017

REFERENCES

- Anderson, A.J., Piltti, K.M., Hooshmand, M.J., Nishi, R.A., and Cummings, B.J. (2017). Preclinical efficacy failure of human CNS-derived stem cells for use in the pathway study of cervical spinal cord injury. *Stem Cell Reports* 8, 249–263.
- Andrews, W., Liapi, A., Plachez, C., Camurri, L., Zhang, J., Mori, S., Murakami, F., Parnavelas, J.G., Sundaresan, V., and Richards, L.J. (2006). Robo1 regulates the development of major axon tracts and interneuron migration in the forebrain. *Development* 133, 2243–2252.
- Arulmoli, J., Wright, H.J., Phan, D.T., Sheth, U., Que, R.A., Botten, G.A., Keating, M., Botvinick, E.L., Pathak, M.M., Zarebinski, T.I., et al. (2016). Combination scaffolds of salmon fibrin, hyaluronic acid, and laminin for human neural stem cell and vascular tissue engineering. *Acta Biomater.* 43, 122–138.
- Baloh, R.H., Tansey, M.G., Lampe, P.A., Fahrner, T.J., Enomoto, H., Simburger, K.S., Leitner, M.L., Araki, T., Johnson, E.M., Jr., and Milbrandt, J. (1998). Artemin, a novel member of the GDNF ligand family, supports peripheral and central neurons and signals



- through the GFRalpha3-RET receptor complex. *Neuron* 21, 1291–1302.
- Basso, D.M., Fisher, L.C., Anderson, A.J., Jakeman, L.B., McTigue, D.M., and Popovich, P.G. (2006). Basso Mouse Scale for locomotion detects differences in recovery after spinal cord injury in five common mouse strains. *J. Neurotrauma* 23, 635–659.
- Bershad, A., Fuentes, M., and Krakauer, D. (2008). Developmental autonomy and somatic niche construction promotes robust cell fate decisions. *J. Theor. Biol.* 254, 408–416.
- Borrell, V., Cardenas, A., Ciceri, G., Galceran, J., Flames, N., Pla, R., Nobrega-Pereira, S., Garcia-Frigola, C., Peregrin, S., Zhao, Z., et al. (2012). Slit/Robo signaling modulates the proliferation of central nervous system progenitors. *Neuron* 76, 338–352.
- Capone, C., Frigerio, S., Fumagalli, S., Gelati, M., Principato, M.C., Storini, C., Montinaro, M., Kraftsik, R., De Curtis, M., Parati, E., et al. (2007). Neurosphere-derived cells exert a neuroprotective action by changing the ischemic microenvironment. *PLoS One* 2, e373.
- Chen, B., Cui, X., Sempowski, G., Domen, J., and Chao, N. (2004). Hematopoietic stem cell dose correlates with the speed of immune reconstitution after stem cell transplantation. *Blood* 103, 4344–4352.
- Cheng, Y.C., Lee, C.J., Badge, R.M., Orme, A.T., and Scotting, P.J. (2001). Sox8 gene expression identifies immature glial cells in developing cerebellum and cerebellar tumours. *Brain Res. Mol. Brain Res.* 92, 193–200.
- Cheng, X., Wang, Y., He, Q., Qiu, M., Whittemore, S.R., and Cao, Q. (2007). Bone morphogenetic protein signaling and olig1/2 interact to regulate the differentiation and maturation of adult oligodendrocyte precursor cells. *Stem Cells* 25, 3204–3214.
- Cummings, B.J., Uchida, N., Tamaki, S.J., Salazar, D.L., Hooshmand, M., Summers, R., Gage, F.H., and Anderson, A.J. (2005). Human neural stem cells differentiate and promote locomotor recovery in spinal cord-injured mice. *Proc. Natl. Acad. Sci. USA* 102, 14069–14074.
- Cummings, B.J., Hooshmand, M.J., Salazar, D.L., and Anderson, A.J. (2009). Human neural stem cell mediated repair of the contused spinal cord: timing the microenvironment. In *From Development to Degeneration and Regeneration of the Nervous System*, C.E. Ribak, C. Aramburo de la Hoz, E.G. Jones, J.A. Larriva Sahd, and L.W. Swanson, eds. (Oxford University Press) <http://dx.doi.org/10.1093/acprof:oso/9780195369007.001.0001>.
- Darsalia, V., Allison, S., Cusulin, C., Monni, E., Kuzdas, D., Kallur, T.S., Lindvall, O., and Kokaia, Z. (2011). Cell number and timing of transplantation determine survival of human neural stem cell grafts in stroke-damaged rat brain. *J. Cereb. Blood Flow Metab.* 31, 235–242.
- Garcia-Alias, G., and Fawcett, J.W. (2012). Training and anti-CSPG combination therapy for spinal cord injury. *Exp. Neurol.* 235, 26–32.
- Garcia-Alias, G., Barkhuysen, S., Buckle, M., and Fawcett, J.W. (2009). Chondroitinase ABC treatment opens a window of opportunity for task-specific rehabilitation. *Nat. Neurosci.* 12, 1145–1151.
- Hamers, F., Lankhorst, A., van Laar, T., Veldhuis, W., and Gispen, W. (2001). Automated quantitative gait analysis during overground locomotion in the rat: its application to spinal cord contusion and transection injuries. *J. Neurotrauma* 18, 187–201.
- Hamers, F., Koopmans, G., and Joosten, E. (2006). CatWalk-assisted gait analysis in the assessment of spinal cord injury. *J. Neurotrauma* 23, 537–548.
- Hargreaves, K., Dubner, R., Brown, F., Flores, C., and Joris, J. (1988). A new and sensitive method for measuring thermal nociception in cutaneous hyperalgesia. *Pain* 32, 77–165.
- Hughes, E., Kang, S., Fukaya, M., and Bergles, D. (2013). Oligodendrocyte progenitors balance growth with self-repulsion to achieve homeostasis in the adult brain. *Nat. Neurosci.* 16, 668–676.
- Iwai, H., Nori, S., Nishimura, S., Yasuda, A., Takano, M., Tsuji, O., Fujiyoshi, K., Toyama, Y., Okano, H., and Nakamura, M. (2014). Transplantation of neural stem/progenitor cells at different locations in mice with spinal cord injury. *Cell Transplant.* 23, 1451–1464.
- Keirstead, H.S., Nistor, G., Bernal, G., Totoiu, M., Cloutier, F., Sharp, K., and Steward, O. (2005). Human embryonic stem cell-derived oligodendrocyte progenitor cell transplants remyelinate and restore locomotion after spinal cord injury. *J. Neurosci.* 25, 4694–4705.
- Koch, U., Lehal, R., and Radtke, F. (2013). Stem cells living with a Notch. *Development* 140, 689–704.
- Koopmans, G.C., Brans, M., Gomez-Pinilla, F., Duis, S., Gispen, W.H., Torres-Aleman, I., Joosten, E.A., and Hamers, F.P. (2006). Circulating insulin-like growth factor I and functional recovery from spinal cord injury under enriched housing conditions. *Eur. J. Neurosci.* 23, 1035–1046.
- Kumamaru, H., Ohkawa, Y., Saiwai, H., Yamada, H., Kubota, K., Kobayakawa, K., Akashi, K., Okano, H., Iwamoto, Y., and Okada, S. (2012). Direct isolation and RNA-seq reveal environment-dependent properties of engrafted neural stem/progenitor cells. *Nat. Commun.* 3, 1140.
- Li, N., and Leung, G.K. (2015). Oligodendrocyte precursor cells in spinal cord injury: a review and update. *Biomed. Res. Int.* 2015, 235195.
- Liew, C.G., Draper, J.S., Walsh, J., Moore, H., and Andrews, P.W. (2007). Transient and stable transgene expression in human embryonic stem cells. *Stem Cells* 25, 1521–1528.
- Liu, C., Chen, B., Deoliveira, D., Sempowski, G., Chao, N., and Storms, R. (2010). Progenitor cell dose determines the pace and completeness of engraftment in a xenograft model for cord blood transplantation. *Blood* 116, 5518–5527.
- Maier, I.C., Ichiyama, R.M., Courtine, G.G., Schnell, L., Lavrov, I., Edgerton, V.R., and Schwab, M.E. (2009). Differential effects of anti-Nogo-A antibody treatment and treadmill training in rats with incomplete spinal cord injury. *Brain* 132, 1426–1440.
- Marsh, S.E., Yeung, S.T., Torres, M., Lau, L., Davis, J.L., Monuki, E.S., Poon, W.W., and Blurton-Jones, M. (2017). HuCNS-SC human NSCs fail to differentiate, form ectopic clusters, and provide no cognitive benefits in a transgenic model of alzheimer's disease. *Stem Cell Reports* 8, 235–248.



- Morrison, B., Cullen, D.K., and LaPlaca, M. (2011). In vitro models for biomechanical studies of neural tissues. In *Neural Tissue Biomechanics*, L.E. Bilston, ed. (Springer), pp. 247–285.
- Nakatsuji, Y., and Miller, R. (2001). Control of oligodendrocyte precursor proliferation mediated by density-dependent cell cycle protein expression. *Dev. Neurosci.* *23*, 356–363.
- Ostenfeld, T., Caldwell, M., Prowse, K., Linskens, M., Jauniaux, E., and Svendsen, C. (2000). Human neural precursor cells express low levels of telomerase in vitro and show diminishing cell proliferation with extensive axonal outgrowth following transplantation. *Exp. Neurol.* *164*, 215–226.
- Piltti, K., Salazar, D., Uchida, N., Cummings, B., and Anderson, A. (2013a). Safety of epicenter versus intact parenchyma as a transplantation site for human neural stem cells for spinal cord injury therapy. *Stem Cells Transl. Med.* *2*, 204–216.
- Piltti, K., Salazar, D., Uchida, N., Cummings, B., and Anderson, A. (2013b). Safety of human neural stem cell transplantation in chronic spinal cord injury. *Stem Cells Transl. Med.* *2*, 961–974.
- Piltti, K.M., Avakian, S.N., Funes, G.M., Hu, A., Uchida, N., Anderson, A.J., and Cummings, B.J. (2015). Transplantation dose alters the dynamics of human neural stem cell engraftment, proliferation and migration after spinal cord injury. *Stem Cell Res.* *15*, 341–353.
- Rosenberg, S., Kelland, E., Tokar, E., De la Torre, A., and Chan, J. (2008). The geometric and spatial constraints of the microenvironment induce oligodendrocyte differentiation. *Proc. Natl. Acad. Sci. USA* *105*, 14662–14667.
- Rossi, S., Nistor, G., Wyatt, T., Yin, H., Poole, A., Weiss, J., Gardener, M., Dijkstra, S., Fischer, D., and Keirstead, H. (2010). Histological and functional benefit following transplantation of motor neuron progenitors to the injured rat spinal cord. *PLoS One* *5*, e11852.
- Salazar, D., Uchida, N., Hamers, F., Cummings, B., and Anderson, A. (2010). Human neural stem cells differentiate and promote locomotor recovery in an early chronic spinal cord injury NOD-scid mouse model. *PLoS One* *5*, e12272.
- Schaar, B.T., Kinoshita, K., and McConnell, S.K. (2004). Doublecortin microtubule affinity is regulated by a balance of kinase and phosphatase activity at the leading edge of migrating neurons. *Neuron* *41*, 203–213.
- Schwarz, Q., and Ruhrberg, C. (2010). Neuropilin, you gotta let me know: should I stay or should I go? *Cell Adh. Migr.* *4*, 61–66.
- Shi, L., Reid, L.H., Jones, W.D., et al. (2006). The microarray quality control (MAQC) project shows inter- and intraplatform reproducibility of gene expression measurements. *Nat. Biotechnol.* *24*, 1151–1161.
- Shi, L., Campbell, G., Jones, W.D., Campagne, F., Wen, Z., Walker, S.J., Su, Z., Chu, T.M., Goodsaid, F.M., Puzstai, L., et al. (2010). The microarray quality control (MAQC)-II study of common practices for the development and validation of microarray-based predictive models. *Nat. Biotechnol.* *28*, 827–838.
- Shuman, S.L., Bresnahan, J.C., and Beattie, M.S. (1997). Apoptosis of microglia and oligodendrocytes after spinal cord contusion in rats. *J. Neurosci. Res.* *50*, 798–808.
- Sontag, C., Nguyen, H., Kamei, N., Uchida, N., Anderson, A., and Cummings, B. (2013). Immunosuppressants affect human neural stem cells in vitro but not in an in vivo model of spinal cord injury. *Stem Cells Transl. Med.* *2*, 731–744.
- Sontag, C., Uchida, N., Cummings, B., and Anderson, A. (2014). Injury to the spinal cord niche alters the engraftment dynamics of human neural stem cells. *Stem Cell Reports* *2*, 620–632.
- Sugimori, M., Nagao, M., Bertrand, N., Parras, C.M., Guillemot, F., and Nakafuku, M. (2007). Combinatorial actions of patterning and HLH transcription factors in the spatiotemporal control of neurogenesis and gliogenesis in the developing spinal cord. *Development* *134*, 1617–1629.
- Tanaka, M., Ohashi, R., Nakamura, R., Shinmura, K., Kamo, T., Sakai, R., and Sugimura, H. (2004). Tiam1 mediates neurite outgrowth induced by ephrin-B1 and EphA2. *EMBO J.* *23*, 1075–1088.
- Teng, J., Takei, Y., Harada, A., Nakata, T., Chen, J., and Hirokawa, N. (2001). Synergistic effects of MAP2 and MAP1B knockout in neuronal migration, dendritic outgrowth, and microtubule organization. *J. Cell Biol.* *155*, 65–76.
- Vasconcelos, F.F., and Castro, D.S. (2014). Transcriptional control of vertebrate neurogenesis by the proneural factor *Ascl1*. *Front. Cell. Neurosci.* *8*, 412.
- Warden, P., Bamber, N., Li, H., Esposito, A., Ahmad, K., Hsu, C., and Xu, X. (2001). Delayed glial cell death following wallerian degeneration in white matter tracts after spinal cord dorsal column cordotomy in adult rats. *Exp. Neurol.* *168*, 213–224.
- Wu, Y., Liu, Y., Levine, E.M., and Rao, M.S. (2003). Hes1 but not Hes5 regulates an astrocyte versus oligodendrocyte fate choice in glial restricted precursors. *Dev. Dyn.* *226*, 675–689.
- Zhou, Q., and Anderson, D.J. (2002). The bHLH transcription factors OLIG2 and OLIG1 couple neuronal and glial subtype specification. *Cell* *109*, 61–73.